THE HYDRODYNAMICS OF RHEOTAXIS IN THE PLAICE (*PLEURONECTES PLATESSA* L.)

By G. P. ARNOLD

Fisheries Laboratory, Lowestoft, Suffolk

AND D. WEIHS

Department of Aeronautical Engineering,
Technion–Israel Institute of Technology, Haifa, Israel

SUMMARY

Plaice resting on the bottom of a flume respond to the current with a clearly defined pattern of behaviour. A simple hydrodynamic model which relates the slip-speed (U_s) and lift-off speed (U_L) to the physical forces acting on the fish has been verified experimentally using freshly killed fish and a rigid model. With an asymmetric semi-ellipsoid shape and a fineness ratio of 14 the plaice appears to be morphologically adapted to have minimum drag when heading into the current. As a result of this streamlined shape the lift force experienced by the fish is 10–20 times greater than the drag force, and the rheotactic behaviour therefore appears to be principally adapted to counteract hydrodynamic lift. Values of U_s and U_L, above which live fish must expend energy against the current, are exceeded for much of each tidal cycle in the southern North Sea. The model is of general application to benthic organisms in flowing water for Reynolds numbers between 10^4 and 10^6; outside these limits some modification of the constants is required.

INTRODUCTION

Plaice (*Pleuronectes platessa* L.) in a flume respond to the current with a clearly defined pattern of rheotactic behaviour, which appears to be of hydrodynamic advantage in maintaining station on the bottom (Arnold, 1969*b*). A simple hydro-dynamic model, which explains the observed behaviour of the fish in quantitative terms, has been developed and tested experimentally using freshly killed and model fish.

THEORY

Behaviour of plaice

In still water on the smooth Perspex bottom of a small flume, plaice usually lie at rest with the whole eyeless surface touching the bottom and both pectoral fins folded flat with their rays closed. The tail is usually spread and respiratory movements are very slight, with only the opercular valve on the ocular side showing any rhythmic movement. At very low current speeds most fish show no response and remain in the

still water posture. Occasionally a raised fin margin is lowered and, rarely, there are a few isolated beats of the marginal fins but there is no increase in respiration rate. As the current speed is increased to 1–2 cm s^{-1} most fish turn to head upstream, generally without leaving the bottom and making the turn by movements of the fins and tail. Some fish remain heading upstream while the speed is further increased but most turn about freely over a range of speeds, even heading downstream at times. When the fish is heading into the current the tail is usually closed and the margins of the fin rays are closely apposed to the bottom. There is a marked increase in the amplitude and frequency of the respiratory movements of the mouth and ocular operculum. Burying movements often occur, particularly after a fish has moved or changed its orientation, and after these a *clamped-down posture* is observed in which the marginal fin rays are pressed tightly against the bottom. At speeds between 20 and 30 cm s^{-1} both facets of behaviour occur more frequently and an *arched-back posture* appears. This develops gradually from the *clamped-down posture* until the back is nearly level for two-thirds of the distance from the ocular pectoral fin to the tail and the inner edges of the marginal fins are raised so that each fin ray is arched steeply up from its tip. A *posterior fin-beating response* also appears in which a wave produced by successive movements of the fin rays travels back along the dorsal and anal fins from apex to tail. When the *arched-back posture* becomes well developed most fish show a vigorous *posterior fin-beating response*, and after several strong beats return to the *clamped-down posture*. With increasing current speed the back becomes progressively more arched and the *posterior fin-beating response* nearly continuous. If the fish is heading along the axis of the current, the beating of the two fins is symmetrical and synchronized but if it is heading diagonally across the axis then usually only the downstream fin shows the response.

At higher speeds the fish begins to be displaced slightly downstream. At first occasional slips of as much as 5 cm are observed to which the fish responds by paddling movements of the marginal fins, moving upstream again and resettling, usually with burying movements. With a further increase in speed slipping becomes more frequent and the fish responds with bursts of swimming clear of the bottom, moving upstream 10–20 cm in each burst. Although they are still capable of swimming upstream against the current for 1–2 m most fish are progressively displaced downstream to the end of the flume and are swept over the weir.

Hydrodynamic analysis

The overall pattern of behaviour suggests that plaice react to the current to avoid being swept away. In stagnant water orientation is random but at rather low speeds most fish turn to head upstream. Theoretically the drag force on the fish should be least in this orientation. A plaice lying on a flat bottom is close to a semi-ellipsoid in shape and for this body the smallest drag is obtained when the long axis is parallel to the flow direction and the blunter end is heading upstream (Hoerner, 1965). This has been confirmed qualitatively by photographing streaklines of particles added to the flow around live plaice (Arnold, 1969b, fig. 6); the least disturbance is obtained when the fish is heading upstream.

The introduction of a semi-ellipsoid body into a uniform stream results in the

acceleration of the flow near to the body. By Bernoulli's law a decrease in pressure occurs on the upper surface, thus:

$$P = P_0 - 0{\cdot}5\rho_s U^2, \tag{1}$$

where P is the local pressure, P_0 is the stagnation pressure obtained by bringing the flow to a halt, ρ_s is the fluid density and U is the local free stream speed. Assuming potential or inviscid flow (i.e. no boundary layer), it can be shown (Lamb, 1963; Weber, 1957) that the flow velocity increases over the front part of the body, reaching its maximum value at the point of maximum thickness. It then decreases symmetrically over the rear part so that the speed is the same at all points on a given horizontal contour on the upper surface of the fish. The pressure along the ventral surface – the stagnation pressure – is constant and higher than that at any point on the dorsal surface so that a lift force is produced. The resultant lift force acts in the vicinity of the geometric centre of the body.

When the negative buoyancy of the fish is exceeded by this vertical lift force the fish will be lifted off the bottom, unless it can produce a downwards force and remain attached to the bottom. Similarly when the viscous drag exceeds the frictional drag between the fish and the bottom the fish will slip downstream. The threshold slipping speed is therefore obtained from

$$D = \mu W, \tag{2}$$

where D is the viscous drag, μ is the static friction coefficient and W is the submerged weight of the fish. As the water speed increases the lift force generated results in a decrease in the submerged weight of the fish so that

$$W = W_0 - L, \tag{3}$$

where W_0 is the submerged weight of the fish in still water and L, the lift force, is defined as

$$L = 0{\cdot}5\rho_s A_f C_L U^2, \tag{4}$$

where ρ_s is the density of the water, A_f is the frontal area of the fish, C_L is the non-dimensional lift coefficient and U is the free stream water speed. The drag is similarly given by

$$D = 0{\cdot}5\rho_s A_f C_{D_0} U^2, \tag{5}$$

where C_{D_0} is the frontal drag coefficient. Substituting equations (2), (4) and (5) into (3) gives an equation for the slip-speed U_s

$$\frac{\rho_s A_f C_{D_0} U_s^2}{2\mu} = W_0 - \frac{\rho_s A_f C_L U_s^2}{2} \tag{6}$$

or after rearrangement,

$$\frac{2W_0}{\rho_s A_f U_s^2} = C_L + \frac{C_{D_0}}{\mu}. \tag{7}$$

Although the values of the individual constants C_L, C_{D_0} and μ are not known for live plaice the quantity $2W_0/\rho_s A_f U_s^2$ is expected to have a constant value for fish of geometrically similar shape and for Reynolds numbers above 10^4, i.e. for fish of at least ʃo cm length with a current speed of more than 10 cm s^{-1}. It is therefore possible to
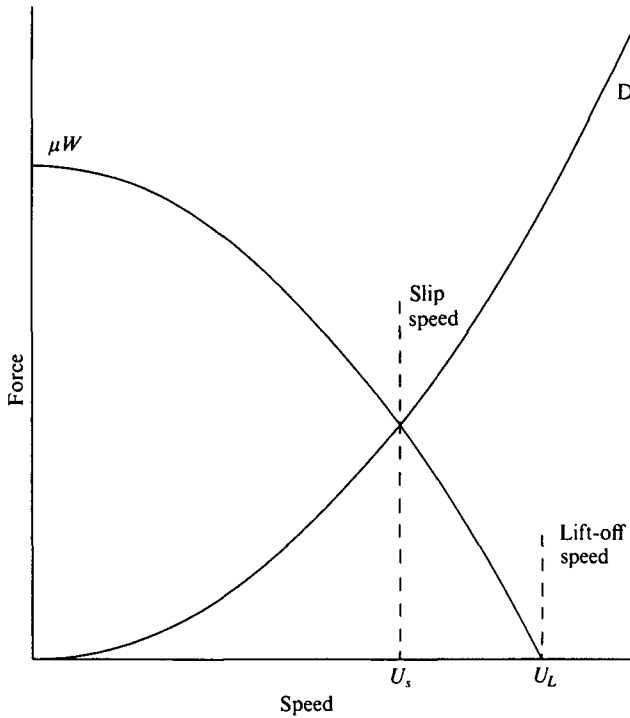
Fig. 1. The hydrodynamic model relating the slip-speed (U_s) and lift-off speed (U_L) to the frictional (μW) and viscous drag (D) forces on the fish.

test this model by measuring W_0, A_f and U_s for fish of a range of sizes and evaluating $2W_0/\rho_s A_f U_s^2$.

The relationship between the frictional and viscous drag forces and the current speed is shown in Fig. 1, from which it can be seen that the model predicts that the fish will slide downstream along the bottom before it lifts off.

MATERIAL AND METHODS

Flume

Circulation system

The experiments were carried out in the flume described by Arnold (1969a). The original recirculating pump has been replaced by a much larger centrifugal pump with a capacity of 126 l s^{-1} at a total generated head of 9·1 m. New steel pipes of 20·3 cm internal diameter lined with epoxy resin have been fitted and the control valves have been replaced with neoprene-coated butterfly valves. A separate cooling system has been installed which recirculates sea water from the sump tank at 0·63 l s^{-1} over a stainless-steel cascade cooler with a capacity of 33 kW. The new recirculating system enables current speeds of up to 1 m s^{-1} to be obtained at the full working depth of 30 cm with the flume in the horizontal mode.

Velocity measurements

The current velocity in the flume was measured with a Kent type 265 Miniflo miniature propeller current meter connected through an electronic emitter-follower circuit to an electronic pulse counter. The meter with a low-speed propeller (no. 6811216) was calibrated in no. 2 Towing Tank at the National Physical Laboratory, Teddington, at speeds between 5 and 100 cm s^{-1} on three occasions between June 1974 and August 1975. The propeller projecting from a strut of aerofoil section was immersed 41 cm below the water surface and the time taken by the carriage to cover a measured 73·15 m was recorded automatically to 0·1 s. The calibration was linear from 5 to 100 cm s^{-1} and the equation of the fitted regression line was $Y = 2\cdot03X - 8\cdot03$, where Y is the pulse counter reading in Hz and X is the current speed in cm s^{-1}.

For the experiments with both the fish and the model the propeller was mounted on the centre line of the first section of the Lowestoft flume, 134·5 cm from the trumpet exit and 10 cm above the bottom. For the flow visualization experiment the propeller was mounted 1 cm from the trumpet exit.

Boundary-layer measurements

The velocity profile in the boundary layer was measured in the middle section of the flume on the centre line with a pitot-static tube of standard NPL design with an ellipsoid nose (Ower & Pankhurst, 1966) and an external diameter of 8 mm. The tip of the tube was set at 283 cm downstream from the trumpet exit and the velocity was measured at 15 heights from 0·4 to 15 cm above the bottom, with free stream speeds of 13·6, 19·3 and 24 cm s^{-1}. A paraffin-filled inclined tube manometer with a scale factor of ×20 was used in conjunction with the twin-reservoir system described by Preston (1972) and the manometer was read to the nearest 0·25 mm. At this point in the flume the velocity profile in the boundary layer has the logarithmic form given by the Karman–Prandtl equation (Prandtl, 1952) for steady two-dimensional flow over a hydrodynamically rough bed:

$$U_z = \frac{U_*}{k} \ln \frac{(z + z_0)}{z_0},$$

where U_z is the current speed at a height z above the bottom, z_0 is the 'roughness length' of the bed and $k = 0\cdot4$ is von Karman's constant. The shear velocity U_* is directly proportional to the linear rate of increase of velocity with log-height and is defined by $U_* = (\tau_0/\rho)^{\frac{1}{2}}$, where τ_0 is the shear stress on the bottom.

At the three free stream speeds of 13·6, 19·3 and 24 cm s^{-1} the equivalent values of the shear velocity U_* in the flume were found to be 0·6, 0·9 and 1·1 cm s^{-1}. At 24 cm s^{-1} with $U_{10} = 20\cdot2$ cm s^{-1} the velocity gradient was described by the equation $\ln z = 0\cdot363U - 5\cdot03$.

Sea water

The experiments with the fish were carried out in October 1974 (fish 1–16), April (fish 17–20) and December (fish 21) 1975 and sea water was obtained from the laboratory's settling tanks. In October 1974 the water in the flume had a salinity of 33·7 ‰

and at the mean temperature of 10·2 °C (range 8·5–13 °C) the density was 1·026 (Hobbs, 1952). In April and December 1975 the salinity was respectively 32·65 and 32·77‰, the mean temperature was between 10 and 11 °C, and in both cases the density was therefore 1·025.

Aeration of the water in the flume occurred progressively during the course of a day's experimental work and the entrained air bubbles were sufficiently small to pass through the apertures (272 μm square) of the fine nylon screen on the trumpet inlet. Experience in the Circulating Water Channel of the National Physical Laboratory's Ship Division at Feltham has shown that the maximum reduction in water density caused by aeration is of the order of 0·25–0·5% (Dr I. W. Dand; personal communication).

Fish

Holding tanks

Details of the experimental fish are given in Table 1. Fish 1–16 were obtained by longshore beam-trawling at Lowestoft and held in the laboratory for about 1 month. Plaice 17–20 were caught by otter trawl in the southern North Sea in December 1974 and were held in the laboratory until April 1975. Plaice 21 was caught by midwater trawl off Lowestoft in December 1975. The fish were held in glass-fibre tanks (92 × 52 × 60 cm height) with a working capacity of 272 l. The bottom of each tank consisted of a biological gravel-bed filter operated by an airlift (Spotte, 1970), which filtered the water in the tank once an hour. In addition a continuous trickle of sea water running to waste changed the water in each tank once every 5 days. The temperature in the holding tanks ranged from 8 to 10 °C and the fish were fed to satiation twice a week on chopped lugworm (*Arenicola marina*).

Measurements

The maximum thickness of each fish was measured to the nearest 0·1 mm using the sliding rod of inverted vernier callipers clamped vertically above a flat perspex plate. The highest point was marked with a small circle of white paper and the fish then photographed on millimetre graph paper. The dimensions x and $2b$ (Fig. 3) were measured from full-size prints of these photographs, and the ocular surface area determined by planimetry. The length of each fish was measured to the nearest 0·5 mm on a conventional measuring board. The fish was then carefully blotted and dried and its weight in air (W_a) measured to the nearest 0·1 g on a Mettler P 1200 balance. Its weight in sea water (W_0) was also measured to the nearest 0·01 g using a conventional balance with a string and hook in place of one of the weighing pans. The string passed through holes in the base of the balance and the bench into a tank filled with sea water of the same density as that in the flume. The balance was zeroed with the hook totally immersed in the water and the fish was then attached to the hook by the point of the jaw. The measurements were made on fish which had been killed in liquid nitrogen and thawed for at least 2 h (see p. 153).

The weight of the fish in air is given by

$$W_a = \rho \chi g, \tag{8}$$

where ρ is the density of the fish, χ its volume and g the acceleration due to gravity. The weight of the fish in still water is given by

$$W_0 = (\rho - \rho_s) \chi g, \tag{9}$$

where ρ_s is the density of the sea water. Substituting equation (8) into (9) and re-arranging gives

$$\rho = \frac{W_a}{(W_a - W_0)} \rho_s. \tag{10}$$

The density and volume of the fish can thus be calculated from the measured values of W_a, W_0 and ρ_s using equations (10) and (8).

Killing the fish in liquid nitrogen results in an initial and significant drop in density but after a period of 1·5–2 h the density returns to within 0·5 % of its original value. This was determined in two ways: first by measuring the density of a single fish over a period of 7·5 h after freezing, and second by comparing the densities of 16 fish initially anaesthetized in MS 222 and subsequently killed in liquid nitrogen.

The single fish ($l = 28·3$ cm; $K = 1·02$, see p. 155) was first anaesthetized in a strong solution of MS 222 and its density determined as 1·068 ($W_a = 230·6$ g wt; $W_0 = 9·38$ g wt; $\rho_s = 1·024$). It was then killed, allowed to thaw in sea water at room temperature and its density redetermined at 1 and 1·5 h after freezing and subsequently at 15 min intervals for a further 6 h. At 1 h after freezing, although both weights had fallen sharply, the volume χ had only increased slightly and the density was found to be 1·056. By 1·5 h both weights had risen again and the density was 1·069. During the ensuing 6 h period while W_a and χ both increased steadily the density was found to fluctuate about a mean value of 1·068 with a coefficient of variation of 0·08 %.

The densities of the 16 plaice ranging in length from 20 to 29 cm ($\overline{K} = 0·87$; s.e. $= 0·01$) were similarly determined after anaesthesia in MS 222 and again at least 2 h after being killed in liquid nitrogen. In each case the density increased and a paired t test (Snedecor & Cochrane, 1967, p. 94) showed that the mean difference in density before and after freezing was $3·21 \times 10^{-3}$ with a standard error of $0·32 \times 10^{-3}$, giving $t = 10$ and $P < 0·001$. The difference in density was thus highly significant but the maximum increase observed after freezing was only 0·5 % and the mean difference was 0·3 %.

Model fish

Two model plaice were cast in Araldite resin (8 parts MY453:1 part HY951 hardener; Ciba (ARL) Ltd) from a mould made of silicone rubber (Silcoset 100; ICI Ltd). The mould was made from a freshly dead fish placed flat on a Perspex sheet with its dorsal, anal and caudal fins spread out and stiffened by a coat of formalin. Liquid Silcoset was poured over the fish to a maximum depth of 3 cm within a cardboard wall surrounding the fish. The first model was cast free, the second stuck to a Perspex plate ($50·6 \times 29·8 \times 0·65$ cm) with the tip of its jaw 20 cm behind the leading edge and its long axis along the centre of the plate. Silcoset was found to be superior to plaster of Paris for making model fish because it gave greater surface detail and because the final mould was flexible. This allowed the finished model to be removed without

breaking off thin undercuts such as the pelvic fins. Shrinkage of the mould during setting was prevented by casting a piece of coarse plastic mesh into the mould above the fish.

The free model had a considerably higher density than a real plaice and with a submerged weight $W_0 = 19.8$ g wt was equivalent to a fish of approximately 25 cm length.

Experimental procedure

Live fish

The behaviour of the live fish was first observed to determine the current velocity at which the *posterior fin-beating response* appeared. Each fish was placed individually in the centre section of the flume heading upstream in still water with the weir at 15 cm height. The fish were confined to this section by grids of 0.8 mm diameter nylon thread with 1 cm square apertures. A slow current was started by opening the control valve (valve 1; Arnold, 1969*a*) a fraction of a turn and then increased by increments of 3–5 cm s^{-1} with 2–3 min at each setting.

Freshly killed fish

Each fish was killed by immersion for 10–15 min in a vessel containing liquid nitrogen (-196 °C) and then thawed in sea water at 10 °C. Fish killed in this way were supple and did not have the swollen lower operculum characteristic of those anaesthetized in MS 222. It was thus possible to ensure that the tip of the jaw touched the bottom as in live fish.

Each freshly killed and thawed fish was placed on the centre line of the central flume section heading upstream with the tip of its jaw 283 cm downstream from the trumpet exit. The weir was again set at 15 cm height. Valve 1 was opened progressively as before to produce incremental increases in velocity of approximately 0.5 cm s^{-1}. At least 1 min was spent at each setting. Three successive determinations were then made of the speed at which each fish slipped back downstream.

Free model fish

The speed at which the free model fish slipped downstream was determined in the same way as for the freshly killed fish. Subsequently a slot ($5.8 \times 2.0 \times 1.5$ cm deep) was milled in the back of the model and filled with lead or polystyrene to alter its weight. The slot, whose front edge was 5 cm behind the nose of the model, was packed with waterproof Plasticene to give a smooth surface flush with the upper surface of the model. The speed of slipping was then remeasured with five different model weights (Table 1).

Flow visualization

To visualize the streamlines over and around the model fish the second model and its baseplate were drilled with a series of 1 mm diameter holes, and sprayed with white paint. A thin box of clear Perspex was glued to the undersurface of the plate and filled with a concentrated solution of potassium permanganate by four tubes at the rear end. These tubes were connected to a reservoir, which was mounted on a vertical screw stand so that the level of solution in it could be raised 1–2 mm above the level
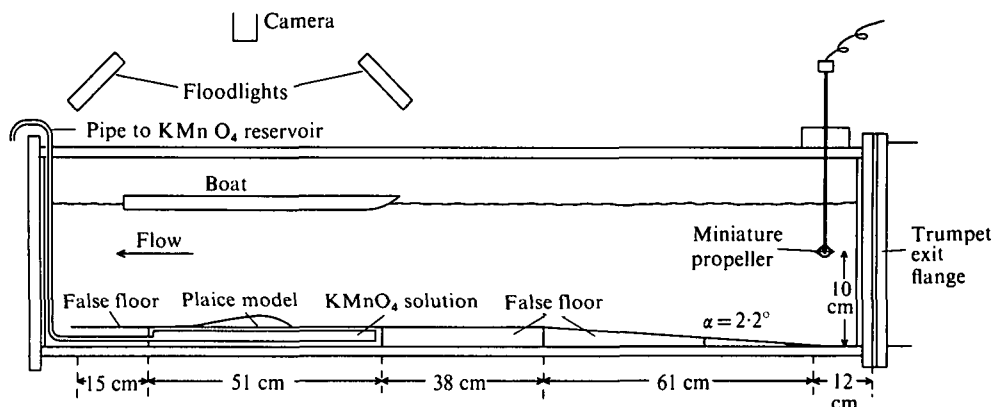
Fig. 2. Apparatus used to visualize the flow patterns round the model plaice.

of the water in the flume. To compensate for the faster flow rate nearer the inlet tubes the holes in the rear half of the plate were drilled out at 0·6 mm diameter. The model was fitted in the first flume section with the top of its baseplate level with a false floor, which had a tapered upstream edge to streamline the flow (Fig. 2).

A fine nylon net (61 μm square apertures) was fitted over the trumpet entrance to remove air bubbles from the water. The streamlines were photographed from above and a boat-shaped tray (61 × 30 × 5 cm wall) of clear Perspex was floated above the model to prevent surface ripples from distorting the image (Fig. 2).

Inclined plane measurements

The static friction coefficient μ was determined both for the model and for freshly killed plaice using an inclined plane of Perspex totally immersed in a bath of still sea water. One end of the Perspex plate was attached to a vertical laboratory screwstand, with which the angle of the plane was smoothly and progressively increased until the fish began to slip down the plane. The coefficient was then given by $\mu = \tan \theta$, where θ was the angle between the plane and the horizontal.

Ten determinations were made of θ for the model fish at each of four weights with W_a = 135, 165, 185 and 215 g wt. Ten determinations of θ were similarly made for seven freshly killed plaice over 30 cm in length. These fish were killed in a very strong solution of MS 222 and did not suffer from a swollen lower operculum. Subsequently they were frozen in liquid nitrogen and thawed – a process which results in the release of copious quantities of mucus. The mucus was then carefully removed from the lower surface by repeated wiping and θ redetermined for each fish.

RESULTS

Fish dimensions

Condition factors

Condition factors were calculated from the expression $K = 100 . W_a . l^{-3}$, where W_a is expressed in g wt and l in cm. Values of K ranged from 0·77 to 1·04 with means of 0·94 for the larger fish (Table 1*a*) and 0·88 for the smaller fish (Table 1*b*) with a

Table 1. *Summary of fish dimensions and displacement speeds*

Fish	l (cm)	h (cm)	b (cm)	x (cm)	l/h	$h/2b$	x/l	A_f (cm²)	W_a (g wt)	W_0 (g wt)	ρ (g cm⁻³)	K	U_s (cm s⁻¹)				$\bar{U}_s$ (cm s⁻¹)	$\dfrac{2W_0}{\rho_s A_f \bar{U}_s^2}$
(a) Freshly killed fish $Re > 10000$																		
1	21.6	1.61	4.1	5.5	13.4	0.20	0.25	10.4	92.7	3.84	1.070	0.91	18.7	18.0	17.7		18.1	2.15
2	20.3	1.54	3.75	4.8	13.2	0.20	0.24	9.1	79.4	3.97	1.080	0.95	22.3	21.5	22.6		22.1	1.71
3	18.1	1.32	3.5	3.0	13.7	0.19	[0.17]	7.3	45.5	2.25	1.079	0.77	22.3	19.6	19.5		20.5	1.41
4	19.3	1.57	3.75	4.6	12.3	0.21	0.24	9.2	73.0	3.70	1.081	1.02	22.1	21.9	22.8		22.3	1.54
5	20.8	1.55	4.0	5.2	13.4	0.19	0.25	9.7	84.4	3.89	1.076	0.94	19.8	17.8	18.7		18.8	2.16
6	31.8	2.32	6.1	8.45	13.7	0.19	0.27	22.2	308.2	12.65	1.070	0.96	21.7	22.4	21.4		21.8	2.28
12	14.7	1.09	2.8	3.85	13.5	0.19	0.26	4.8	30.7	1.82	1.090	0.97	18.9	18.7	17.9		18.5	2.12
13	15.3	1.16	2.95	4.2	13.2	0.20	0.27	5.4	33.3	1.97	1.091	0.93	18.8	19.6	19.6		19.3	1.88
14	14.4	1.08	2.85	—	13.3	0.19	—	4.8	31.0	1.81	1.089	1.04	19.2	16.2	23.0		19.5	1.89
15	15.8	1.14	2.87	3.5	13.9	0.20	0.22	5.1	36.3	1.90	1.083	0.92	21.9	21.5	—		21.7	1.50
16	14.4	1.09	2.65	3.6	13.2	0.21	0.25	4.5	27.8	1.73	1.094	0.93	19.5	20.9	20.1		20.2	1.78
17	36.6	2.54	7.2	8.7	14.4	0.18	0.24	28.7	415.5	18.6	1.074	0.85	21.1	22.7	—		21.9	2.58
18	30.4	2.32	6.4	7.55	13.1	0.18	0.25	23.3	290.6	13.62	1.075	1.03	24.9	23.9	23.5		24.1	1.93
19	32.0	2.28	6.3	7.3	14.0	0.18	0.23	22.6	285.5	12.28	1.071	0.87	22.3	23.6	23.4		23.1	1.95
20	39.8	3.07	7.2	9.2	13.0	0.21	0.23	34.7	631.8	25.53	1.068	1.00	22.6	27.0	24.1		24.6	2.33
21	50.8	3.82	9.15	10.8	13.3	0.21	0.21	54.9	1137.4	54.34	1.076	0.91	28.8	29.0	34.8		31.4	1.92
													35.2	30.4	30.4			
Mean					13.4	0.20	0.24				1.079	0.94						1.95
S.E.					0.1	0.003	0.005				0.002	0.02						0.08
(b) Freshly killed fish $Re < 10000$																		
7	6.5	0.44	1.2	1.65	14.8	0.18	0.25	0.8	2.5	(0.12)	—	0.92	15.9	12.8	12.0		13.5	1.50
8	6.6	0.45	1.25	1.6	14.7	0.18	0.24	0.9	2.4	(0.11)	—	0.83	14.9	14.4	15.5		14.9	1.07
9	8.2	0.56	1.5	2.0	14.6	0.19	0.24	1.3	4.6	(0.21)	—	0.84	16.4	16.0	16.3		16.2	1.15
10	7.0	0.53	1.3	1.8	13.2	0.20	0.26	1.1	3.1	(0.15)	—	0.91	17.4	17.3	18.0		17.6	0.86
11	6.0	0.43	1.1	1.55	13.9	0.19	0.26	0.7	2.0	(0.09)	—	0.91	16.3	18.3	18.2		17.6	0.75
Mean					14.2	0.19	0.25					0.88						1.07
S.E.					—	0.004	0.003					0.02						0.13
(c) Model fish $Re > 10000$																		
7	22.7	1.78	5.0	7.0	12.7	0.18	0.31	14.0	148.7	19.85	1.184	0.92	34.3	37.2	38.1	38.5	37.0	1.98
									181.5	52.76	1.446	0.83	54.8	53.9	56.5	54.6	54.9	2.39
									197.1	68.17	1.568	0.84	61.2	61.3	62.0	61.0	61.4	2.48
									222.1	93.02	1.765	0.91	69.9	73.1	71.7	71.8	71.6	2.49
									157.7	28.73	1.254		40.9	41.2	41.0	—	41.0	2.34
									145.9	16.73	1.159		33.3	30.1	31.4	31.4	31.5	2.30
											Mean	0.88						2.3
											S.E.	0.02						0.07

standard error of 0·02 in each case. Dawes (1930, 1931) found that values of K ranged from 0·6 to 1·1 for recently caught plaice with the majority in the range 0·8–1·0, so that the experimental fish were representative of wild fish.

Density

The densities of the large experimental fish were found to have a mean value of 1·079 (Table 1*a*) with a standard error of 0·002, which after applying a correction of 0·3 (see p. 153) represents a mean density of 1·076 prior to freezing. This value is similar to the densities for the plaice of 1·0655 ('five small specimens') to 1·0884 ('one large specimen') given by Lowndes (1942, 1955) and determined by the displacement method in which the volume of the organism is measured directly.

The values of W_0 and χ shown in Table 1*b* for the smaller fish were calculated from the measured values of W_a assuming a density of 1·076.

Geometry

In most of the experimental fish the point of maximum thickness occurred in the small triangle bounded by the posterior edge of the skull, the edge of the folded ocular pectoral fin and the curve of the lateral line as indicated by the open circle in Fig. 3. Table 1 shows that for these fish the ratio x/l had a mean value of 0·25. In a few fish the upper surface of the ocular operculum was more curved than usual and its height was close to h. In fish 3 the point of maximum thickness was on the operculum at $x/l = 0·17$ and this value has been excluded in calculating the mean value of x/l given in Table 1.

In the fish from which the models were cast the position of maximum thickness was relatively further back at $x/l = 0·31$ with $l = 22·7$ cm. Fig. 3 shows a plan of the free model together with its sagittal and transverse sections. The transverse section $(C–D)$ is shown at the point of maximum width $2b$ $(x'/l = 0·33)$, which had the same thickness as h. The cross-sectional area of section $C–D$ was measured by planimetry and found to be 13·65 cm². A semi-ellipse with the same values of h and b is shown superimposed on the section CD in Fig. 3. Its cross-sectional area is given by $A = 0·5\,\pi hb$ so that with $h = 1·78$ cm and $b = 5$ cm, $A = 13·96$ cm², which is within 2·5 % of the measured cross-sectional area of the model. It is clear from the ratios l/h, $h/2b$ and x/l in Table 1 that the experimental fish were all geometrically similar to the model. The frontal area A_f of each experimental fish was therefore calculated from $A_f = 0·5\,\pi hb$, and the results are shown in Table 1 and in Fig. 4*a* plotted against length squared. The fitted regression line has the equation $A_f = 0·0216l^2 + 0·28$.

Fig. 4*b* similarly shows the relation between ocular surface area and length squared. The two curves show the total area, including the marginal fins and tail, and the smaller area of the body and peduncle. The fitted regression lines have the equations $A_t = 0·2977l^2 + 0·17$ and $A_b = 0·2008l^2 + 0·13$, respectively. In fish 6 the marginal fins were somewhat folded, resulting in an underestimate of total area. The aspect ratio (AR) of each fish was calculated from $\mathrm{AR} = 4b^2/A_b$, where A_b was the body area measured by planimetry. The aspect ratio of the 21 experimental fish was found to have a mean value of 0·71 with a standard error of 0·008. Maximum thickness was related to length by the regression $h = 0·074l$. In both longitudinal and transverse sections, therefore, the plaice is close to a semi-ellipsoid in shape with thickness:
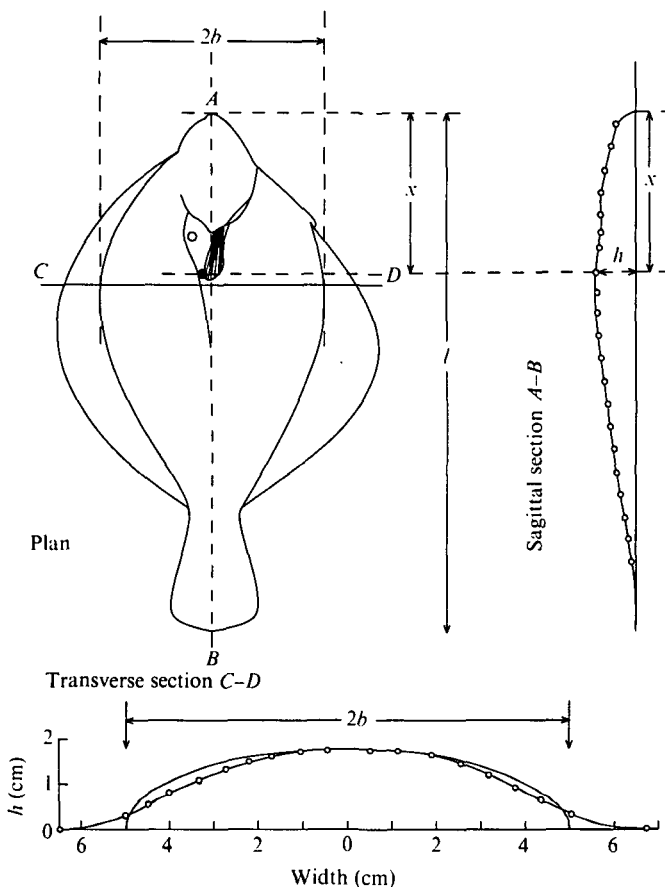
Fig. 3. Geometry of the plaice.

length ratios respectively of $l/h = 13\cdot6$ and $h/2b = 0\cdot2$ and an overall aspect ratio of $0\cdot7$.

Flow patterns

The flow patterns round the model plaice are shown in Fig. 5. This demonstrates clearly the stagnation point that occurs just in front of the jaw and the flow separation over the rear of the fish, which is indicated by backflow. As separation appears only close to the tail Weber's (1957) analysis of the flow around a semi-ellipsoid can be used for theoretical calculations of plaice hydrodynamics, when the fish is resting on the bottom. Weber (1957) gives the relation between the aspect ratio and the velocity increment ΔU on the upper surface for several values of the ratio $h/2b$. Taking $h/2b = 0\cdot2$ (Table 1 a) and the aspect ratio as $0\cdot7$ it can be seen from Weber's fig. 12 that the velocity increment ΔU on the uppermost point of the plaice is $\Delta U \simeq 0\cdot1\ U$, where U is the free-stream velocity at height h. For any value of U the velocity on the upper surface of a plaice is thus increased by 10 %, resulting in a pressure decrease of approximately 20 %, which produces the hydrodynamic lift postulated in the theoretical approach. The presence of lift is also seen from the streamwise vortices shed from the
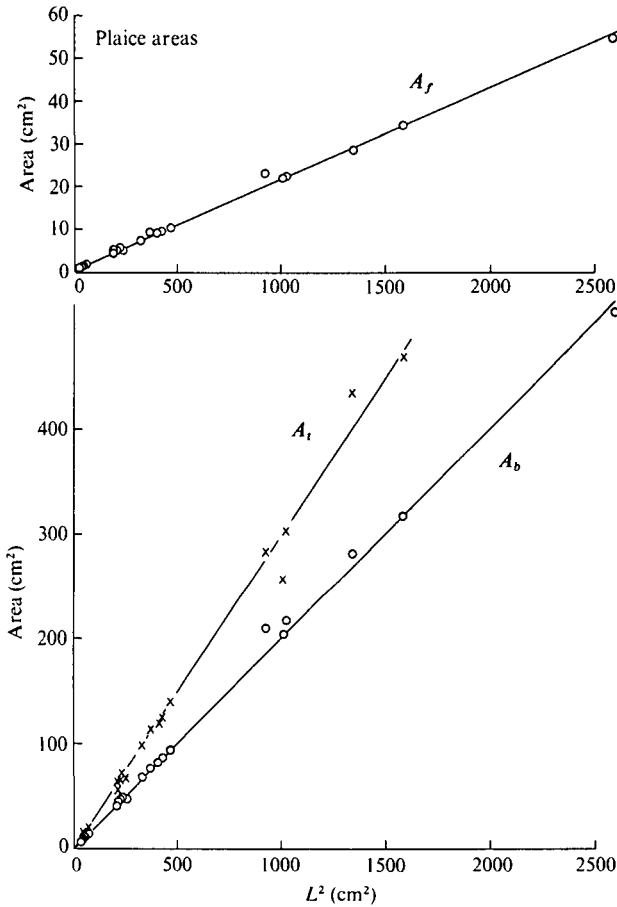
Fig. 4. Relation between length and area of plaice. A_f is the projected frontal area, A_t the total ocular surface area and A_b the ocular surface area less the area of the dorsal, anal and caudal fins.

fin tips indicated by the streamwise concentration of dye. These vortices are of the 'leading edge' type observed in slender-wing aircraft such as Concorde (AR < 1).

Test of hydrodynamic model

The measurements of the slip-speed U_s showed that within the limits of experimental error the non-dimensional quantity $2W_0/\rho_s A_f \bar{U}_s^2$ was a constant with a value of approximately 2 for both the model and the freshly killed fish.

Measurement errors

The maximum error in the determination of $2W_0/\rho_s A_f \bar{U}_s^2$ resulting from errors in the measurements of the physical dimensions of the fish was of the order of $\pm 1\%$ so that the greatest source of error was in the measurement of the slip speed U_s. The overall coefficient of variation for the values of U_s in Table 1 (a) was 5·2% so that the resultant error in $2W_0/\rho_s A_f \bar{U}_s^2$ was of the order of $\pm 10\%$.

There were several problems in measuring U_s. Firstly, the end-point could only be determined by increasing the speed of the water and not by decreasing it. Secondly, the fish did not always slip smoothly and on several occasions both fish and model jerked back 1–2 mm at one or two increments of speed below that at which they slipped properly downstream. Thirdly, the fish were in the boundary layer and the propeller was (deliberately) in free stream, so that a small change of speed at the fish was reflected by a larger change at the propeller. Fourthly, although great care was taken to align both the fish and the model along the axis of the flume, they occasionally rotated slowly as they began to slip. The model, for example, rotated as it began to slip during each of the four determinations of U_s when $W_0 = 19.85$ g wt and fish 11 did the same at $U_s = 16$ cm s^{-1}, whilst subsequently it slipped straight downstream at $U_s = 18$ cm s^{-1} (Table 1a). When the rotation clearly occurred before slipping the measurement was rejected but when the fish turned as it slipped the measurements were included in the data. Frequently both fish and model began to rotate after they had slipped several centimetres downstream and, while still sliding, were hydro-dynamically unstable, often beginning to stall and flip over.

Another problem arose with the freshly killed fish. The tip of the jaw sometimes came 1–2 mm off the bottom during the 15–20 min required for each set of measurements and a fish in this posture slipped at a somewhat lower speed than when the tip of its jaw was in contact with the bottom. This occurred with fish 14 and 20 at speeds of 16 and 22 cm s^{-1} but the effect of raising the head was most clearly seen in fish 21, which was a ripe female with a full ovary and therefore a somewhat swollen lower surface. Six determinations of U_s were made for this fish and all are shown in Table 1 (a). For the first two measurements the tip of its jaw was between 2 and 5 mm off the bottom and the fish slipped at $U_s = 29$ cm s^{-1}, whilst in the next two observations the jaw was touching the bottom and the fish did not slip until $U_s = 35$ cm s^{-1}. In the fifth determination the fish lifted directly off the bottom at 30 cm s^{-1} without slipping while in the last observation it slipped downstream at $U_s = 30$ cm s^{-1} but only partially lifted off the bottom.

Table 1 shows the free stream current speeds at which each of the 21 freshly killed fish first slipped downstream along the bottom of the flume. For 8 of these fish the total range between the maximum and minimum values of U_s was less than 1 cm s^{-1}. For a further 8 fish the range was between 1–2 cm s^{-1} and for the remaining 5 it was greater than 2 cm s^{-1}. For fish 3, 7, 14, 20 and 21 the difference was respectively 2.8, 3.9, 6.9, 4.4 and 6.4 cm s^{-1}.

Freshly killed fish, Reynolds number $Re > 10^4$

The quantity $2W_0/\rho_s A_f U_s^2$ was calculated for each fish and each determination of U and the results are shown in Fig. 6(a) plotted against log W_0 for the 16 larger fish, where $Re > 10^4$. The corresponding values of $2W_0/\rho_s A_f \bar{U}_s^2$ are shown in Table 1(a) and Fig. 6(b). Values of $2W_0/\rho_s A_f U_s^2$ ranged from 1.2 to 2.8 with a mean of 1.96 and a standard error of 0.05. The equivalent 95% confidence limits are 1.86 and 2.06 and are within the limits of 1.76 and 2.16 to be expected from the 10% error in determining U_s^2. It was concluded therefore that the quantity $2W_0/\rho_s A_f \bar{U}_s^2$ was a constant with a value of about 2.
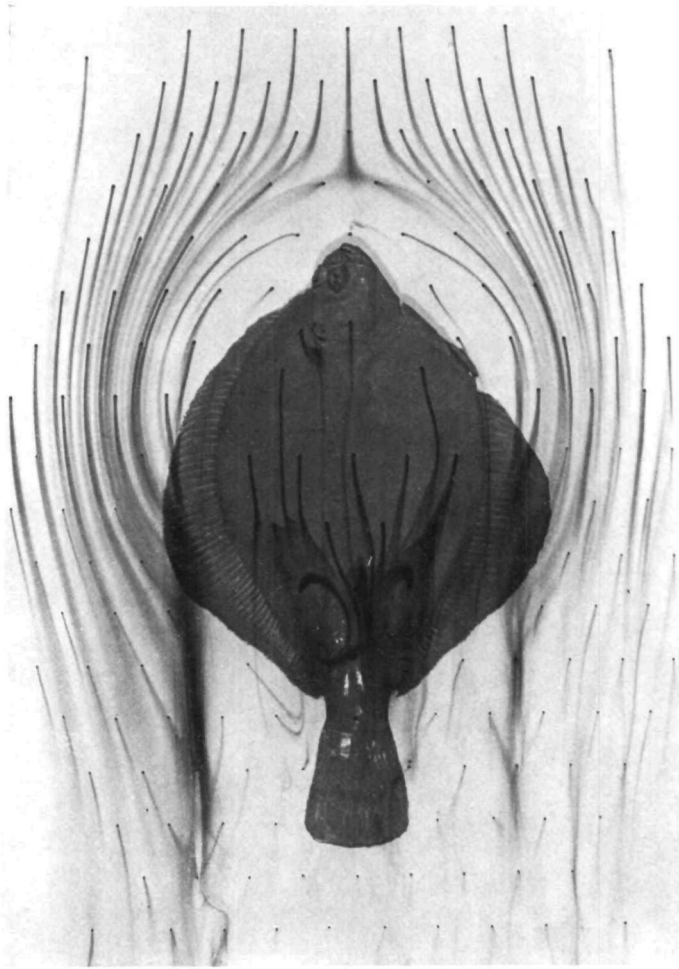
Fig. 5. Flow patterns round the model plaice with $U_{10} = 10$ cm s^{-1}
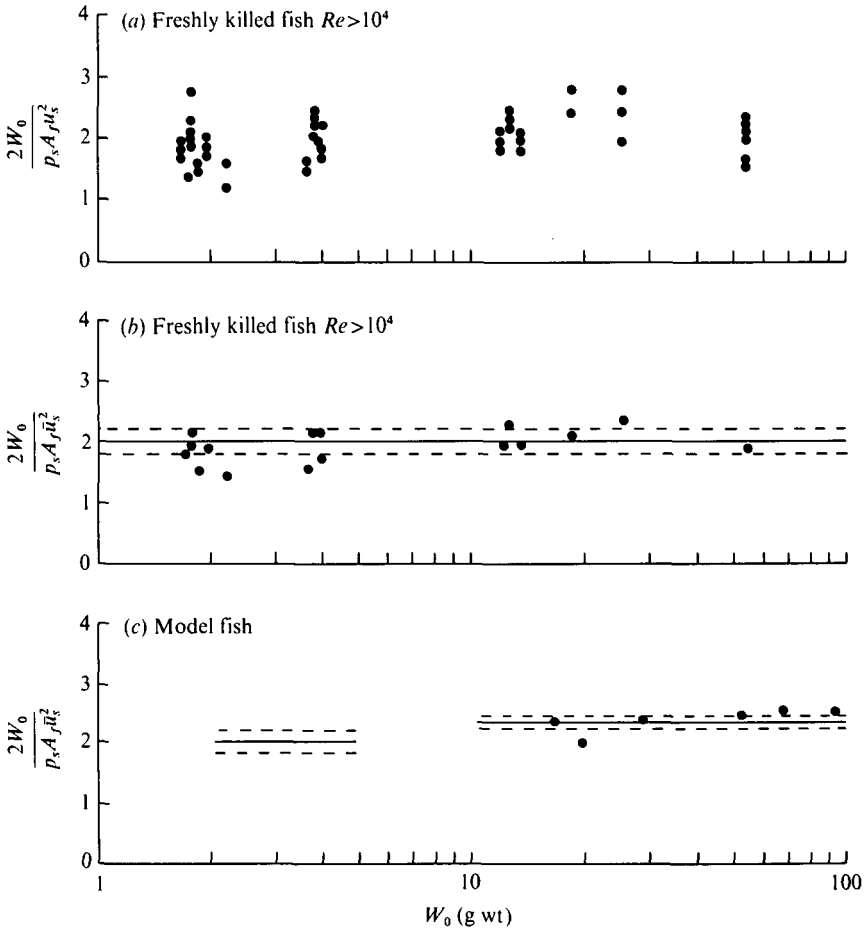(Reynolds number, $Re = 2 \cdot 3 \times 10^4$).

Fig. 6. Test of the hydrodynamic model. The relation between $2W_0/\rho_s A_f U_s^2$ and log W_0 for the freshly killed fish over 10 cm in length and for the model fish.

Model fish

The hydrodynamic model was further tested by measuring the slip speed of the model fish and systematically varying its weight while keeping A_f constant. Six weights were used and the corresponding values of U are given in Table 1 (c). The mean value of $2W_0/\rho_s A_f U_s^2$ for the model was 2·3 with a standard error of 0·04. The corresponding values of $2W_0/\rho_s A_f \bar{U}_s^2$ are shown in Fig. 6(c) plotted against log W_0. The equivalent 95 % confidence limits were 2·24 and 2·42, which again are within the limits of 2·1 and 2·56 expected from the 10 % error in determining U_s^2.

A t test showed that the mean value of $2W_0/\rho_s A_f U_s^2$ for the model was significantly greater than that of 1·96 for the freshly killed fish ($t = 5\cdot5$; $P < 0\cdot001$), suggesting that the model was not entirely comparable with the real fish (see p. 163). However, when the mean value of $2W_0/\rho_s A_f U_s^2$ for the model is compared with that (2·1, S.E. 0·07) for the 6 larger fish for which $W_0 > 10$ g then the difference is no longer significant. This suggests that there is perhaps a slight trend in the value of $2W_0/\rho_s A_f \bar{U}_s^2$

Table 2. *Static friction coefficients (μ) for freshly killed and mucus-free plaice*

(θ is the angle of the plane to the horizontal at which the fish began to slide.
See text for further details.)

	Freshly killed fish		Mucus-free fish	
L (cm)	θ (deg)	μ	θ (deg)	μ
39·7	12·6	0·22	37·7	0·77
35·9	14·4	0·26	—	—
40·2	10·8	0·19	35·8	0·72
38·6	6·1	0·11	37·9	0·78
37·4	12·2	0·22	39·4	0·82
39·2	10·8	0·19	34·0	0·68
32·9	22·6	0·42	31·5	0·61
Mean	12·8	0·23	36·1	0·73
S.E.	1·9	0·03	1·2	0·03

with W_0 and that experiments with a model of less than 10 g wt would give a somewhat lower value of $2W_0/\rho_s A_f \bar{U}_s^2$.

Freshly killed fish, Reynolds number Re $<$ 10^4

The values of $2W_0/\rho_s A_f U_s^2$ for the freshly killed fish under 10 cm in length ranged from 0·7 to 1·9. A t test showed that the mean value of 1·08 was significantly different ($t = 8\cdot6$; $P < 0\cdot001$) from that of 1·96 for the larger fish in Table 1(a). It was clear that, as predicted, the model did not apply where $Re < 10^4$ for which the equation should be of the form

$$C_L + \frac{C_{D_0}}{\mu} = \frac{2W_0}{\rho_s A_f U_s^{2-\delta(l)}}, \tag{11}$$

where δ is a function of the length of the fish (Hoerner, 1965).

For Reynolds numbers of 10^3–10^4, δ is smaller than 0·3 (Weihs, 1977). Recalculating the non-dimensional factor $C_L + C_{D_0}/\mu$ with $\delta = 0\cdot2$ for fish 7–11 (Table 1b) gives values ranging from 1·3 to 2·5, close to those of the larger fish.

Hydrodynamic coefficients

Static friction coefficient

As expected there was no significant difference in the values of μ determined for the weighted and unweighted model fish, and taking all the measurements together it was found that μ had a mean value of 0·49 with a standard error of 0·01. Table 2 summarizes the results of the experiments with the freshly killed fish, for which it was found that μ had a mean value of 0·23 with a standard error of 0·03. For the mucus-free fish μ was over three times as large, with a mean value of 0·73. Those fish which were used to test the hydrodynamic model (Table 1) were killed in liquid nitrogen and released copious quantities of mucus. While the surplus mucus was removed with absorbent paper before use, none was wiped dry, and it is reasonable to assume that for these fish μ was of the order of 0·2–0·4.

Lift and drag coefficients

Because the lift and drag coefficients should be calculable from equation (7) using the experimentally determined values of μ and $2W_0/\rho_s A_f \bar{U}_s^2$ and because of the practical difficulties involved, no attempt was made to measure directly the values of C_L and C_{D_0}. It was found, however, that taking $C_L + C_{D_0}/0.2 = 1.95$ for the fish (Table 1a) and $C_L + C_{D_0}/0.5 = 2.3$ for the model (Table 1c) that $C_L = 2.5$ and $C_{D_0} = -0.12$. The negative value of C_{D_0} shows that the model was not completely comparable with the real fish and the most probable reasons for this were its lack of flexibility and somewhat rougher surface.

Nevertheless, given its geometry it is possible to obtain an independent estimate of C_{D_0} for the plaice. The drag of an asymmetric semi-ellipsoid body resting on a flat surface with its blunt end heading upstream is a function of its fineness ratio l/h (Hoerner, 1965). For minimum drag the optimum value lies between 10 and 15 and for the plaice $l/h = 13.6$ (Table 1). The corresponding minimum drag coefficient is of the order of 0.03 but, depending on the boundary layer thickness, surface roughness and the width of its trailing edge, the actual value of C_{D_0} for a body of this type can vary between 0.04 and 0.08. Allowing for the roughness of the eyes and nasal papillae on the head of the plaice, and for the drag resulting from lift, it is reasonable to assume a total frontal drag coefficient of the order of 0.08–0.16. Taking $C_L + C_{D_0}/\mu = 2$ for the fish, the equivalent values of C_L range from 1.2 to 1.8 with $\mu = 0.2$ to $\mu = 0.4$. The corresponding lift coefficient for the model with $C_L + C_{D_0}/\mu = 2.3$ and $\mu = 0.5$ is $C_L = 2$.

The ratio of C_L/C_{D_0} for the plaice thus falls in the range 7.5–22.3 and the lift force experienced by the fish heading upstream on the bottom of the flume is of the order of 10–20 times greater than the drag force.

Slip speeds and lift-off speeds

To maintain its position on the bottom a plaice must expend energy against the forces produced on it by the current. Fig. 1 shows that because it is negatively buoyant the plaice does not have to produce a forward thrust until the current reaches the slip-speed U_s and the viscous drag exceeds the frictional drag between the fish and the bottom. Similarly it does not have to produce a downwards force until the lift force exceeds W_0 at the lift-off speed U_L. Between U_s and U_L it is therefore working solely against drag.

The slip speed U_s is defined by equation (7) and taking $C_L + C_{D_0}/\mu = 2$ it follows that $U_s^2 = W_0/\rho_s A_f$. At the lift-off speed the lift force L equals the submerged weight W_0 so that U_L is similarly defined by equation (4) and $U_L^2 = 2W_0/\rho_s A_f C_L$. The ratio of the two speeds is therefore given by $U_s/U_L = 0.7\sqrt{C_L}$.

The slip speeds of plaice of standard lengths from 10 to 50 cm have been calculated from these equations taking $\rho_s = 1.026$, the mean annual value for the southern North Sea (ICES, 1962), together with equivalent lift-off speeds using three values of C_L in the range 1.2–1.8. The submerged weight W_0 of each fish was calculated from the regression $\ln W_a = 3.02 \ln l - 4.74$, determined from the data in Table 1, and equation (10). The frontal area was calculated from the regression $A_f = 0.0216$

Table 3. *Calculated speeds at 10 cm above the bottom of the flume (U_{10}) at which freshl■ killed plaice slip downstream (U_s) and are lifted off the bottom (U_L)*

l (cm)	W_a (g wt)	W_0 (g wt)	A_f (cm²)	U_s (cm s⁻¹)	U_L (cm s⁻¹)		
					$C_L = 1·0$	$C_L = 1·4$	$C_L = 1·8$
10	9·1	0·42	2·44	12·8	18·1	15·3	13·5
20	74·1	3·45	8·92	19·2	27·2	23·0	20·2
30	252·2	11·72	19·72	23·8	33·7	28·5	25·1
40	601·2	27·94	34·84	27·7	39·2	33·1	29·2
50	1179·3	54·8	54·28	31·1	43·9	37·1	32·7

Table 4. *Current speeds at which live fish showed movements of the posterior marginal fins*

Fish	Fins raised (cm s⁻¹)	Incipient beating (cm s⁻¹)	Continuous beating, V (cm s⁻¹)	$\bar{U}_s$ (cm s⁻¹)	$V/\bar{U}_s$
1	—	—	19·2	18·1	1·06
2	—	—	20·9	22·1	0·95
3	—	—	23·7	20·5	1·16
4	—	—	21·7	22·3	0·97
5	—	—	21·9	18·8	1·16
6	25·3	—	—	21·8	—
7	—	15·9	27·0	13·5	2·00
8	—	—	17·0	14·9	1·14
9	5·6	—	12·1	16·2	0·75
10	—	1–2	23·8	17·6	1·35
11	—	—	18·8	17·6	1·07
12	7·6	18·5	23·6	18·5	1·27
13	—	—	26·6	19·3	1·38
14	—	—	22·7	19·5	1·16
15	—	18·2	23·7	21·7	1·09
16	—	13·3	23·7	20·2	1·17
17	—	—	30·9	21·9	1·41
18	—	—	27·2	24·1	1·13
19	17–20	—	27·4	23·1	1·19
20	—	13·6	21·4	24·6	0·87

$l^2 + 0·28$ (Fig. 4a). The values of U_s and U_L are shown in Table 3, from which it can be seen that, as the lift coefficient increases, U_L decreases until it is equal to U_s when $C_L = 2$. It is of interest therefore to note that on one occasion fish 21 lifted directly off the bottom without first slipping downstream.

Live fish

The behaviour of the live plaice was the same as that described by Arnold (1969b) and summarized above. It was observed in addition that the pigmentation of the ocular surface of several fish became progressively darker during stages 2 and 3 of the behaviour pattern. This was interpreted as a stress response comparable to that described in cod by Harden Jones & Scholes (1974).

Table 4 summarizes the current speeds at which the *posterior fin-beating respons■*

appeared in each fish. A distinction is made between continuous beating of the marginal fins and an incipient form of the response in which only the last few rays of either fin showed a few slight movements. This incipient form invariably occurred at a lower current speed than the continuous beating, in the case of fish 10 at between 1 and 2 cm s^{-1}. Continuous beating generally occurred between 20 and 30 cm s^{-1}, with a lower speed in a few instances, and an average speed of 23 cm s^{-1}. Table 4 also shows the mean slip speed $\bar{U}_s$ of each fish taken from Table 1 and the ratio of the speed V of continuous beating to the slip speed. The ratio ranged from 0·75 to 2·0 with a mean value of 1·2, but its value was less than 1·0 for only 4 of the 19 fish involved and for 3 of these it was between 0·9 and 1·0. For the remainder, with the exception of fish 7, the ratio fell between 1·0 and 1·4. Fish 7 was unusual in that continuous beating did not appear until the current speed had reached twice the slip-speed. Since it has been shown above that the ratio U_L/U_s falls in the range 1–1·4 ($C_L = 1$ to $C_L = 2$) it can be concluded that in the majority of fish continuous beating of the posterior marginal fins first occurs in the speed range U_s to U_L. Fish 6 was unusual in that it never showed the response, instead merely raising the posterior marginal fins and allowing water to flow underneath it. Three other fish also raised their posterior marginal fins at lower speeds but subsequently showed the fin-beating response at higher speeds.

DISCUSSION

The optimal shape for a streamlined body in free flow is one which gives it the minimum drag for maximum volume and this is obtained when the fineness ratio l/d is approximately 4, where d is the maximum diameter of the body (Hoerner, 1965; Hertel, 1966; Webb, 1975). For fast swimming fish and dolphins l/d falls within 10% of the optimum (Hertel, 1966), although in practice it is found that the ratio can vary between 3 and 7 and only result in about a 10% increase in drag from the minimal value (Webb, 1975). In addition, tuna and dolphins show a remarkable similarity to a modern laminar wing profile and have the point of maximum thickness set well back along the body at x/l from 0·5 to 0·7 (Hertel, 1966). In contrast, the optimal shape for an external fairing on an aeroplane or a plane wall is an asymmetric ellipsoid with the blunt end pointing upstream (Hoerner, 1965). Minimal drag is obtained when the fineness ratio l/h is two to three times the corresponding optimal ratio of l/d for a streamlined body in free flow and has a value between 10 and 15. With $l/h = 14$ and $x/l = 0·24$ the body shape of the plaice thus gives it minimal drag when resting on a hard bottom and heading into the current. It is concluded that this is a morphological adaptation which parallels that of the fast free-swimming fish outlined above and this conclusion raises interesting questions of evolution.

Flatfish are generally thought to have evolved from some marine percoid ancestor that adopted the habit of resting on one side (Verrill, 1897; Norman, 1934) and this habit is found today in such families as the Seranidae and Labridae. The tautog (*Tautoga onitis*), for example, commonly rests on its side on the bottom of aquaria (Verrill, 1897) and small specimens have been observed in this posture on the sea-bed in a state of winter torpor (Olla, Bejda & Martin, 1974). All the available evidence suggests that the flatfishes, which comprise the Order Heterosomata, form a homo-

Table 5. *The fineness ratios of the plaice and other flatfish compared with those of* Psettodes, *perch and other round fish*

Species		Author	l/d	l/h	x/l
Tuna	*Euthynnus affinis*	Magnuson (1970) (*l* excludes keel)	4·0	4·9	0·5
Rainbow trout	*Salmo gairdneri*	Hertel (1966)	5·4	7·3	0·39
Whiting	*Gadus merlangus*	Haslett (1962)	6·5	8·9	0·24
Perch	*Perca fluviatilis*	Kipling (1957)	5·1	7·5	0·3
—	*Psettodes erumei*	Norman (1934)	5·1	12·3	—
Halibut	*Hippoglossus hippoglossus*	de Groot (1970)	4·6	12·2	—
Greenland halibut	*Reinhardtius hippoglossoides*	de Groot (1970)	5·8	12·3	—
Plaice	*Pleuronectes platessa*	de Groot (1970)	4·4	15·2	—
Plaice	*Pleuronectes platessa*	(Table 1)	4·4	13·6	0·24

geneous group derived from a generalized percoid ancestor and that *Psettodes*, the least specialized genus, represents an intermediate evolutionary stage (Norman, 1934). It is instructive, therefore, to compare the fineness ratio of the plaice with those of the perch, *Psettodes*, and a number of other species (Table 5). For fish in which the two dimensions h and $2b$ differ significantly the fineness ratio l/d is calculated for an equivalent spindle, where $d = (h+2b)/2$ (Hertel, 1966).

A number of interesting points emerge from Table 5. The first is that the ratio l/h for the flatfish is between 1·6 and 2 times that for the perch. The second is that *Psettodes*, with $l/h = 12·3$, is clearly very much nearer to the flatfish than it is to the perch, so that in this particular aspect of its morphology it is probably not intermediate between the flatfish and their generalized percoid ancestor. This may reflect the fact that it is thought to spend a great deal of its time lying on the bottom (Norman, 1934) and suggests that the development of the semi-ellipsoid shape was perhaps the first and most important step in the evolution of asymmetry with the other morphological adaptations developing later. The final point is that for all the fish in Table 5 the ratio l/d falls within the range for which the volume drag coefficient approaches the optimal value.

As a result of its shape, the lift force on a plaice resting on a flat bottom and heading upstream is of the order of 10–20 times the drag force and represents a significant percentage of the fish's submerged weight, rising rapidly with current speed to equal W_0 at U_L. It can be argued therefore that the *posterior fin-beating response* is primarily a mechanism for reducing the vertical pressure differential across the fish and this is consistent with the observation that the response first appears in the majority of live fish at speeds between U_s and U_L, and in some individuals at speeds a little below U_s. In the *clamped-down posture* the marginal fin rays are pressed against the bottom and seal off the lower surface but once the back is arched and these fins are raised water can enter the space beneath the fish through the gap between mouth and anus. At lower speeds some fish are observed in this posture with water flowing beneath them (Arnold, 1969b, fig. 2), while at higher speeds the *posterior fin-beating response* has been shown to be a pumping mechanism producing an appreciable velocity beneath the fish (Arnold, 1969b, fig. 7). By Bernoulli's law this will reduce the pressure on the lower surface, oppose the lift force on the ocular surface and therefore increase the slip-speed of the live fish above that of the freshly killed one. At the slip-speed U_s the

drag force $D = \mu(W_0 - L)$, so that, if at speeds up to U_L the fish can produce a downwards force equal and opposite to the lift force, it can make $|D| = |\mu W_0|$ and $|U_s| = |U_L|$.

The fact that the water is pumped out downstream by the *posterior fin-beating response* also has hydrodynamic significance. From pressure-reducing requirements only the direction in which water is expelled is unimportant, because the relevant parameter U^2 is a scalar quantity. But if the fish is to keep station with minimum effort the drag force must be minimized. Pumping water out against the external current not only incurs a higher expenditure of energy but also produces a large flow disturbance leading to a higher total drag so that a fish heading downstream incurs the highest possible drag penalty. In any other orientation both effects are reduced and are minimal when the fish is heading upstream, when in addition the pumping of the posterior marginal fins also generates a forward thrust opposed to the viscous drag force tending to displace the fish downstream. The fact that only the downstream fin is used when the fish is heading across the flow can also be interpreted as a drag-reduction mechanism.

At lower speeds some fish develop the *arched-back posture* while keeping the ends of all the marginal fins in contact with the bottom. It is thought that the blind side of pleuronectids is capable of acting as a suction disc on smooth surfaces (Grenholm, 1923; Orcutt, 1950), so that possibly, in such circumstances, the plaice can oppose the lift force produced by the current by a hydrostatic mechanism such as is used by littoral marine fish (Gibson, 1969), rather than by the hydrodynamic one outlined above. Measurements of the velocity and pressure beneath the fish would be required to resolve this point.

It seems clear that both morphologically and behaviourally the plaice is highly adapted to life on the sea-bed in a tidal environment. It is instructive, therefore, to compare the values of U_s and U_L for plaice of the various sizes shown in Table 3 with current speeds that commonly occur in the sea. There are few data on speeds at 10 cm above the bottom but McCave (1973) has measured velocity profiles near the sea-bed at various sites in the southern North Sea and calculated the equivalent values of U_{10}. At station 9 on the West Hinder Bank measurements made over a 13 h tidal cycle in August 1969 (I. N. McCave, personal communication) showed that, with a surface velocity rising to a maximum of 98 cm s^{-1}, U_{10} exceeded 20 cm s^{-1} for 9 h, 30 cm s^{-1} for 4·8 h and 35 cm s^{-1} for 3 h. For a period of about 12 min U_{10} exceeded 40 cm s^{-1} reaching a maximum of 42 cm s^{-1}. Clearly therefore all the slip-speeds and most of the lift-off speeds shown in Table 3 are exceeded for much of the tidal cycle. On the western side of the North Sea off the East Anglian coast tidal speeds are consistently higher. At neap tides values of U_{10} of 20, 30 and 40 cm s^{-1} are exceeded for 52, 15 and 1 % of each tidal cycle. At spring tides the equivalent values are 78, 63 and 38 % and off Southwold, with a peak speed of $U_{100} = 104$ cm s^{-1} and a shear velocity $U_* = 7·2$ cm s^{-1}, U_{10} can reach 70 cm s^{-1} for short periods (Dickson & Medler, 1978). Even off Texel, where current speeds are generally much slower, McCave's measurements showed that U_{10} exceeded 20 cm s^{-1} for 7 h out of a 13 h tidal cycle, reaching a maximum of 32 cm s^{-1} with a surface velocity of 60 cm s^{-1}.

McCave's data for Texel and West Hinder showed that with values of U_{10} of 20 and 22 cm s^{-1} the equivalent shear velocities were o·8 and 1·8 cm s^{-1} respectively, which compare with values of o·9 and 1·1 cm s^{-1} at free stream speeds of 19·3 and

24 cm s^{-1} in the flume. With $U_{10} = 20$ cm s^{-1} the speeds experienced by a 40 cm plaice at 3 cm above the bottom would be 16·9 and 16·4 cm s^{-1} with values ot U_* of 1·1 and 1·84. With such close agreement in shear velocity the comparison of the experimental values of U_{10} with those for the North Sea is clearly valid.

When a shallow layer of sand is provided in the flume one of the first responses of the fish to the current, if it has not already done so in still water, is to bury and remain buried until the sand is eroded from around it (Arnold, 1969b). This occurs at quite low speeds and thereafter the fish shows the same behaviour as on a hard flat bottom. With values of U_{10} of 20–40 cm s^{-1} frequently occurring in the southern North Sea it seems possible that, unless it is able to bury more deeply in the sea-bed than it usually does in laboratory tanks, or can take shelter in the lee of sand waves, burying might only enable plaice to avoid the current for relatively short periods of each tidal cycle around slack water.

It has recently been shown (Greer Walker, Harden Jones & Arnold, 1978) that acoustically tagged plaice can spend as much time in midwater as on the bottom, and it appears from the fineness ratios in Table 5 that flatfish are morphologically adapted to have minimum drag, not only when resting on the bottom, but also when swimming freely. On the other hand the plaice has one of the highest densities and sinking factors of all marine fish (Harden Jones & Marshall, 1953) and to stay up in midwater must produce a lift force equal to W_0. With a reasonable angle of attack, however, a plaice would probably only need to swim at a speed of 10–20 cm s^{-1} relative to the water to obtain the necessary lift (Lighthill in Harden Jones, 1977), so that its density may not be the disadvantage that it first appears. Indeed it could actually save energy in midwater if the plaice were able to utilize its negative buoyancy by swimming in an alternate swimming and gliding mode (Weihs, 1973). High density could then be regarded as an adaptation to both pelagic and benthic phases of the life history.

The hydrodynamic model developed in this paper is of general application to all benthic organisms in flowing water. As described above (p. 162), the theory requires some modification at Reynolds numbers less than 10^4, where transitional effects occur. Other modifications of the constants may be required at Reynolds numbers of the order of 10^6 and above (i.e. beyond the range of interest for fish up to 1 m in length), because of different flow mechanisms in this range.

REFERENCES

ARNOLD, G. P. (1969a). A flume for behaviour studies of marine fish. *J. exp. Biol.* **51**, 671–679.
ARNOLD, G. P. (1969b). The reactions of the plaice (*Pleuronectes platessa* L.) to water currents. *J. exp. Biol.* **51**, 681–697.

DAWES, B. (1930). Growth and maintenance in the plaice (*Pleuronectes platessa* L.). Part I. *J. mar. biol. Ass. U.K.* **17**, 103–174.

DAWES, B. (1931). Growth and maintenance in the plaice (*P. platessa* L.). Part II. *J. mar. biol. Ass. U.K.* **17**, 877–947.

DICKSON, R. R. & MEDLER, K. J. (1978). Boundary layer tidal currents in the southern North Sea and English Channel. *J. Cons. int. Explor. Mer* (in preparation).

GIBSON, R. N. (1969). Powers of adhesion in *Liparis montagui* (Donovan) and other shore fish. *J. exp. mar. Biol. Ecol.* **3**, 179–190.

GREER-WALKER, M. G., HARDEN JONES, F. R. & ARNOLD, G. P. (1978). Movements of plaice (*Pleuronectes platessa* L. (tracked in the open sea. *J. Cons. int. Explor. Mer.* **38**, 58–86.

GRENHOLM, Å. (1923). Studien über die Flossenmuskulatur der Teleostier. *Uppsala Univ. Årsskr.* **2**, 1–296.

GROOT, S. J. DE (1970). Some notes on ambivalent behaviour of the Greenland halibut *Reinhardtius hippoglossoides* (Walb.) Pisces: Pleuronectiformes. *J. Fish. Biol.* **2**, 275–279.

HARDEN JONES, F. R. (1977). Performance and behaviour on migration. In *Fisheries Mathematics* (ed. J. H. Steele). London: Academic Press.

HARDEN JONES, F. R. & MARSHALL, N. B. (1953). The structure and functions of the teleostean swimbladder. *Biol. Rev.* **28**, 16–83.

HARDEN JONES, F. R. & SCHOLES, P. (1974). The effect of low temperature on cod, *Gadus morhua*. *J. Cons. int. Explor. Mer* **35**, 258–271.

HASLETT, R. W. G. (1962). Measurement of the dimensions of fish to facilitate calculations of echostrength in acoustic fish detection. *J. Cons. int. Explor. Mer* **27**, 261–269.

HERTEL, H. (1966). *Structure–Form–Movement.* New York: Reinhold.

HOBBS, A. (1952). *Tables for Sea Water Density.* U.S. Navy Hydrographic Office, Washington, D.C. Publication 615.

HOERNER, S. F. (1965). *Fluid-dynamic Drag.* Midland Park, New Jersey: Hoerner.

ICES (1962). *Mean Monthly Temperature and Salinity of the Surface Layer of the North Sea and Adjacent Waters from 1905 to 1954.* ICES Service Hydrographique, Charlottenlund Slot.

KIPLING, C. (1957). The effect of gill-net selection on the estimation of weight–length relationships. *J. Cons. int. Explor. Mer* **23**, 51–63.

LAMB, H. (1963). *Hydrodynamics.* Cambridge University Press.

LOWNDES, A. G. (1942). The displacement method of weighing living aquatic organisms. *J. mar. biol. Ass. U.K.* **25**, 555–574.

LOWNDES, A. G. (1955). Density of fishes. Some notes on the swimming of fish to be correlated with density, sinking factor and load carried. *Ann. Mag. nat. Hist.* **8**, 241–256.

MAGNUSON, J. J. (1970). Hydrostatic equilibrium of *Euthynnus affinis*, a pelagic teleost without a gas bladder. *Copeia*, pp. 56–85.

McCAVE, I. N. (1973). Some boundary-layer characteristics of tidal currents bearing sand in suspension. *Mém. Soc. r. Sci. Liège* **6**, 187–206.

NORMAN, J. R. (1934). *A Systematic Monograph of the Flatfishes (Heterosomata).* Vol. I. *Psettodidae, Bothidae, Pleuronectidae.* London: British Museum.

OLLA, B. L., BEJDA, A. J. & MARTIN, A. D. (1974). Daily activity, movements, feeding, and seasonal occurrence in the tautog, *Tautoga onitis. Fish. Bull. nat. mar. Fish. Serv. U.S.* **72**, 27–35.

ORCUTT, H. G. (1950). The life history of the starry flounder, *Platichthys stellatus* (Pallas). *Fish. Bull. Calif.* (78), 7–64.

OWER, E. & PANKHURST, R. C. (1966). *The Measurement of Air Flow.* Oxford: Pergamon Press.

PRANDTL, L. (1952). *Essentials of Fluid Dynamics.* London: Blackie.

PRESTON, J. H. (1972). The measurement of pressure in low velocity water flows. *J. Phys. (E. Sci. Instrum.)* **5**, 277–282.

SNEDECOR, G. W. & COCHRANE, W. G. (1967). *Statistical Methods*, 6th ed. Iowa State University Press.

SPOTTE, S. H. (1970). *Fish and Invertebrate Culture.* New York: Wiley-Interscience.

VERRILL, A. E. (1897). Nocturnal and diurnal changes in the colors of certain fishes and of the squid (Loligo), with notes on their sleeping habits. *Am. J. Sci.* **3**, 135–136.

WEBB, P. W. (1975). Hydrodynamics and energetics of fish propulsion. *Bull. Fish. Res. Bd Can.* (190), 1–159.

WEBER, J. (1957). The calculation of the pressure distribution on thick wings of small aspect ratio at zero lift in subsonic flow. *Rep. Memo. aeronaut. Res. Comm. (Counc.)* (2993), 1–45.

WEIHS, D. (1973). Mechanically efficient swimming techniques for fish with negative buoyancy. *J. mar. Res.* **31**, 194–209.

WEIHS, D. (1977). Effects of size on sustained swimming speeds of aquatic organisms. In *Scale Effects of Animal Locomotion* (ed. T. J. Pedley), pp. 333–338. London: Academic Press.